Electronic Supplementary Information

White-light-emitting single MOF sensor based array for berberine homologues discrimination

Qian Wang, Qiao Liu, Xiao-Meng Du, Bo Zhao, Yue Li* and Wen-Juan Ruan*

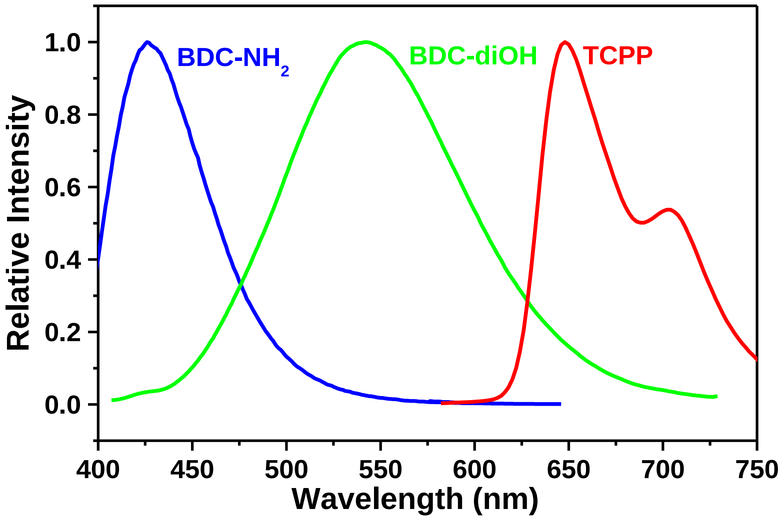

Fig. S1 Fluorescent spectra of free BDC-NH_2, BDC-diOH and TCPP ligands, λ_{em} = 388 nm.

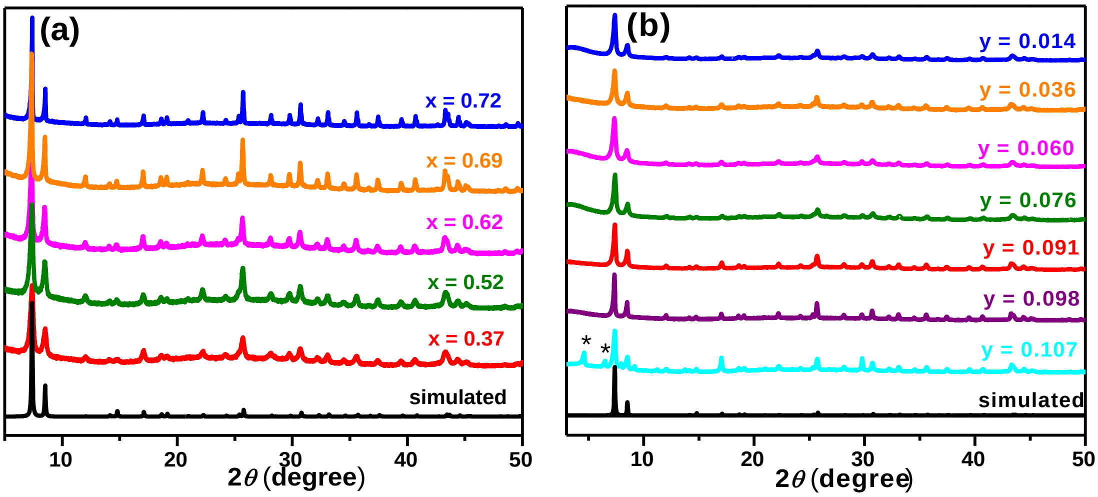

Fig. S2 PXRD patterns of (a) UiO-66-$(NH_2)_x(diOH)_{1-x}$ and (b) $TCPP_y$⊂UiO-66-$(NH_2)_{0.62}(diOH)_{0.38}$ samples. The diffraction peaks of impurity phase are marked by "*".

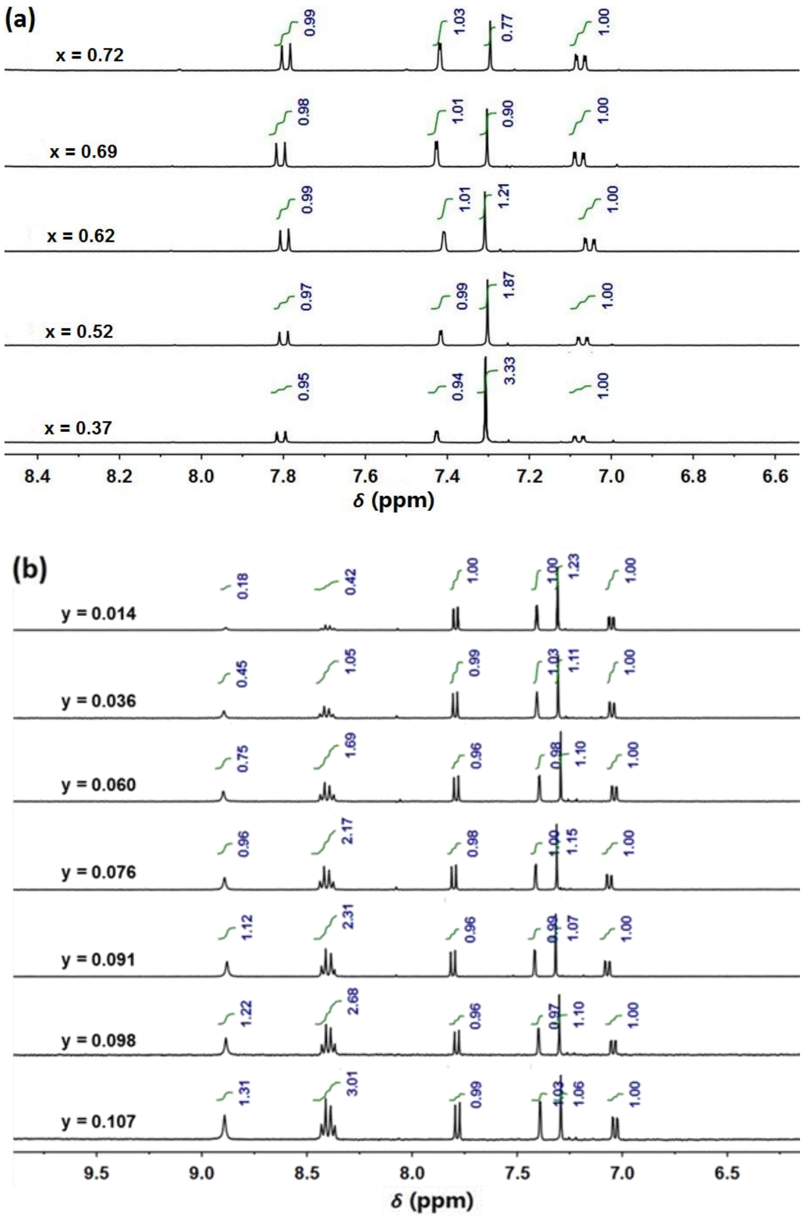

Fig. S3 ^{1}H NMR spectra of digested solutions of (a) UiO-66-$(NH_2)_x(diOH)_{1-x}$ and (b) $TCPP_y \subset$UiO-66-$(NH_2)_{0.62}(diOH)_{0.38}$ with dilute HF in DMSO-d_6. BDC-NH_2 δ: 7.08 (d, J = 8.0 Hz, 1H), 7.42 (s, 1H), 7.78 (d, J = 7.6 Hz, 1H). BDC-diOH δ: 7.30 (s, 2H). δ: 8.40 (q, 16H), 8.90 (s, 8H).

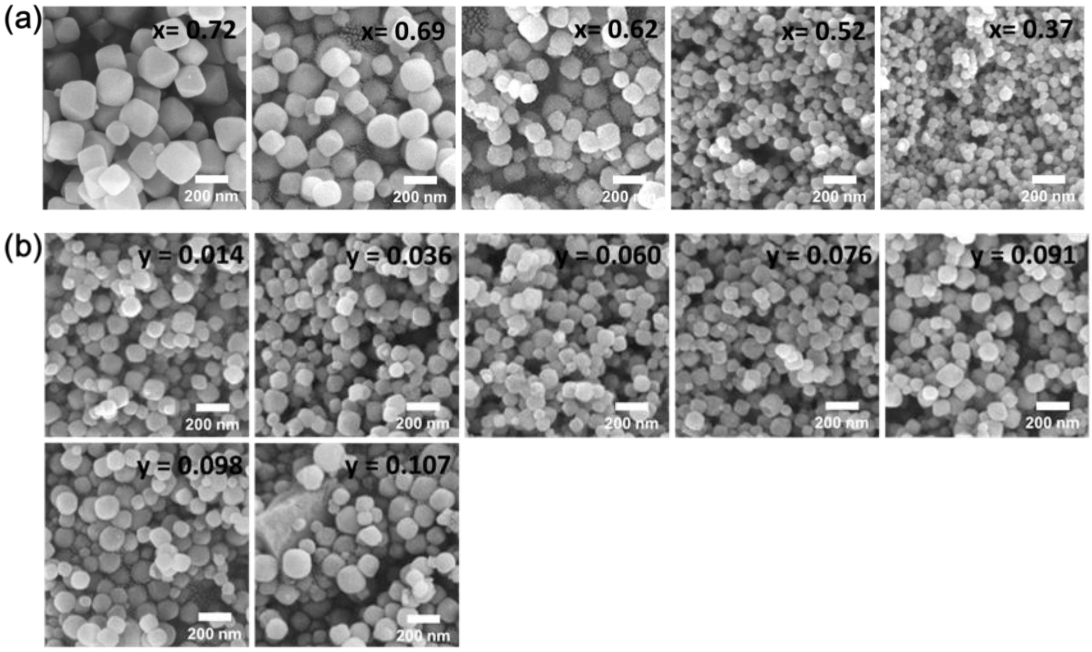

Fig. S4 SEM images of (a) UiO-66-$(NH_2)_x(diOH)_{1-x}$ and (b) $TCPP_y \subset$UiO-66-$(NH_2)_{0.62}(diOH)_{0.38}$ samples.

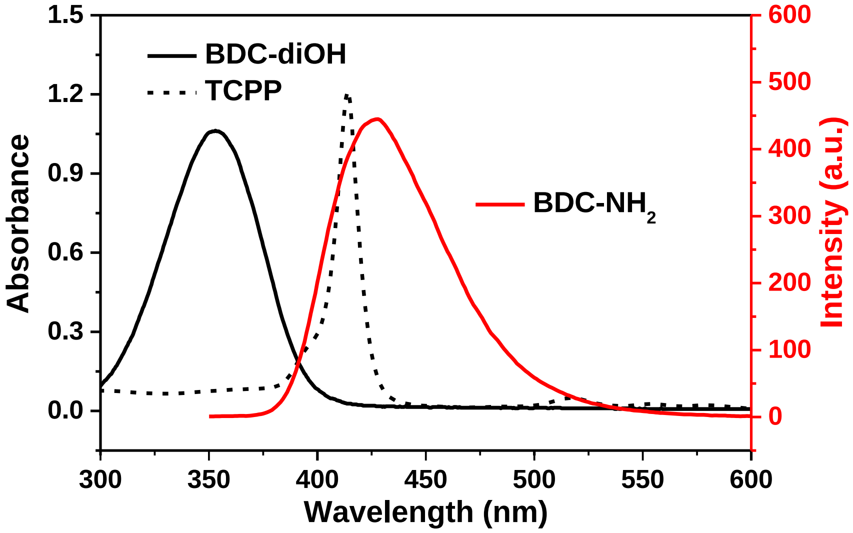

Fig. S5 Comparison of the emission spectrum of BDC-NH_2 with the absorption spectra of BDC-diOH and TCPP.

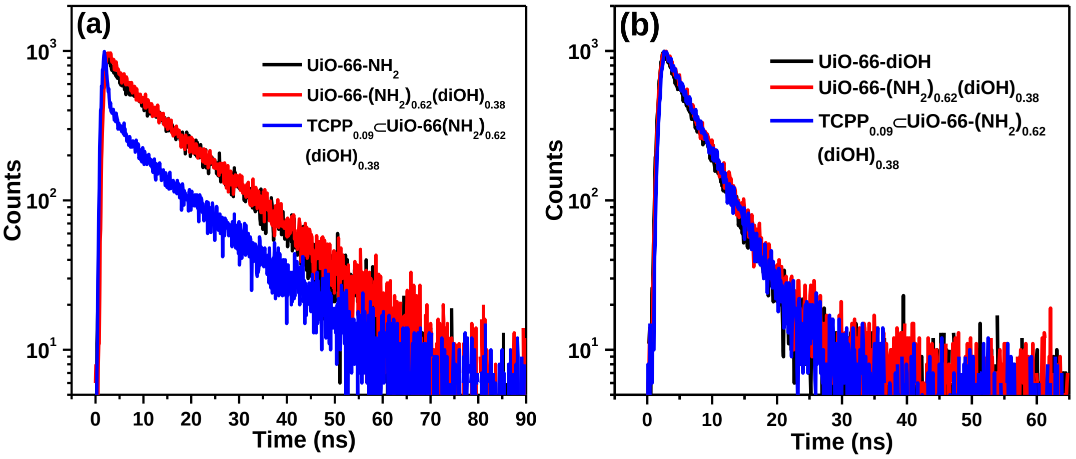

Fig. S6 Time-resolved decays of the emission bands at (a) 440 and (b) 536 nm.

The emission band at 440 nm comes from the fluorescence of BDC-NH$_2$ ligand. The decays of this band in UiO-66-NH$_2$ and UiO-66-(NH$_2$)$_{0.62}$(diOH)$_{0.38}$ could be satisfactorily fitted to single-exponential kinetics with the lifetimes of 15.6 and 15.7 ns, respectively. After the incorporation of TCPP, this band presented a biexponential decay with a major term with longer lifetime (τ_1 = 14.9 ns, 90.5%) and a minor subnanosecond term (τ_2 = 0.8 ns, 9.5%). The average lifetime of these two terms was 13.6 ns. The emission band at 536 nm comes from BDC-diOH. The decay kinetics of this component was single-exponential and gave nearly the same lifetime in UiO-66-diOH (4.7 ns), UiO-66-(NH$_2$)$_{0.62}$(diOH)$_{0.38}$ (4.7 ns) and TCPP$_{0.09}$⊂UiO-66-(NH$_2$)$_{0.62}$(diOH)$_{0.38}$ (4.8 ns).

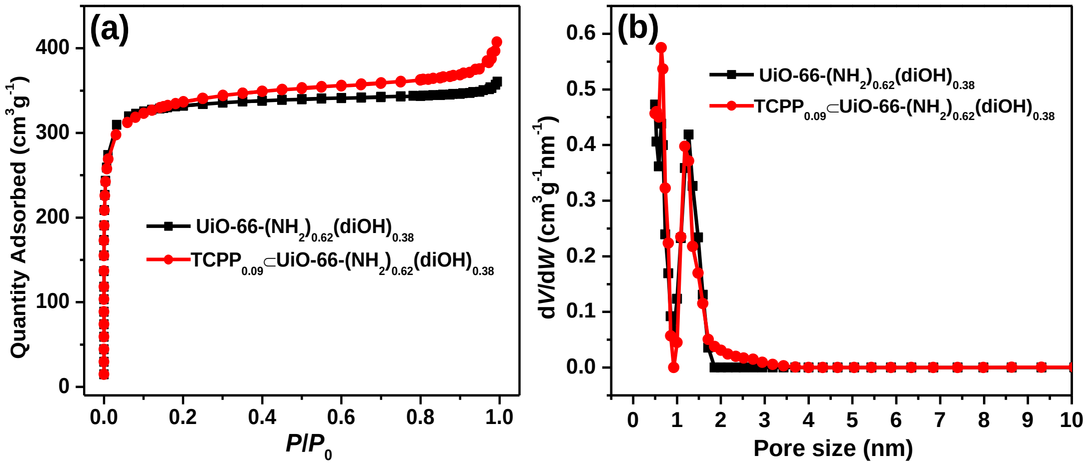

Fig. S7 (a) N_2 adsorption isotherms (at 77 K) and (b) BJH pore-size distribution curves of UiO-66-$(NH_2)_{0.62}(diOH)_{0.38}$ and $TCPP_{0.09}$⊂UiO- 66-$(NH_2)_{0.62}(diOH)_{0.38}$.

With above isotherms, the BET surface areas of UiO-66-$(NH_2)_{0.62}(diOH)_{0.38}$ and $TCPP_{0.09}$⊂UiO-66-$(NH_2)_{0.62}(diOH)_{0.38}$ were calculated to be 1084 and 1045 m^2 g^{-1}, respectively, and their pore volumes were 0.409 and 0.414 cm^3 g^{-1}. The apertures of these two samples are in the range of 0.5–2 nm, so their pores belong to micropore.

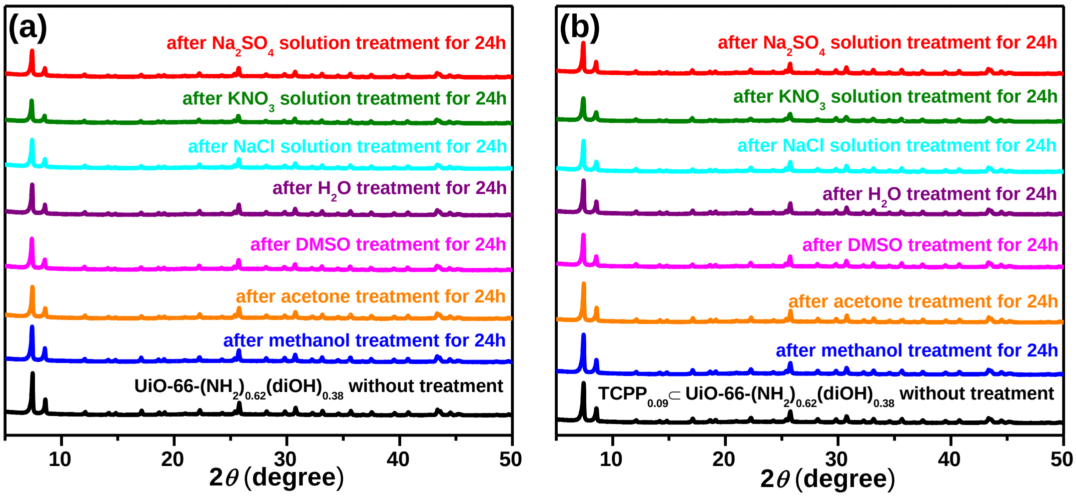

Fig. S8 PXRD patterns of the (a) UiO-66-$(NH_2)_{0.62}(diOH)_{0.38}$ and (b) $TCPP_{0.09}$⊂UiO-66-$(NH_2)_{0.62}(diOH)_{0.38}$ samples immersed in different organic solvents and saturated salt solutions.

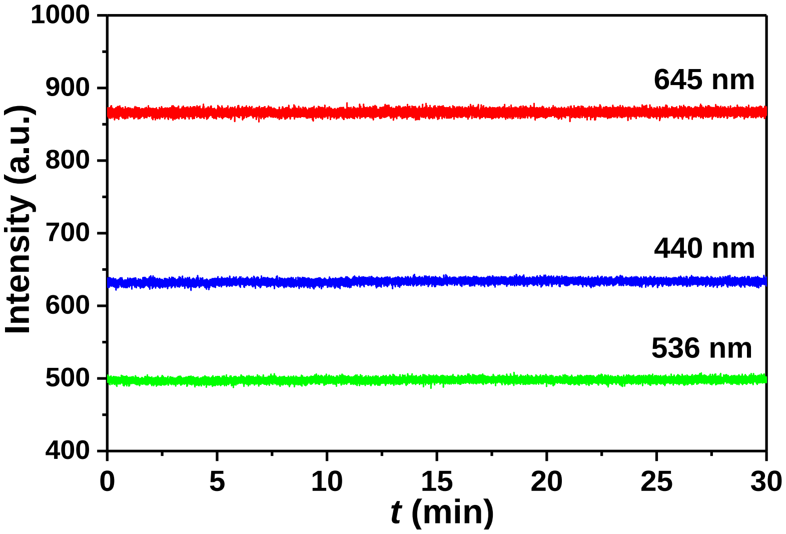

Fig. S9 Temporal change of the fluorescent intensities at 440, 536 and 645 nm with prolonging measurement of $TCPP_{0.09}\subset UiO\text{-}66\text{-}(NH_2)_{0.62}(diOH)_{0.38}$ suspension, λ_{ex} = 388 nm.

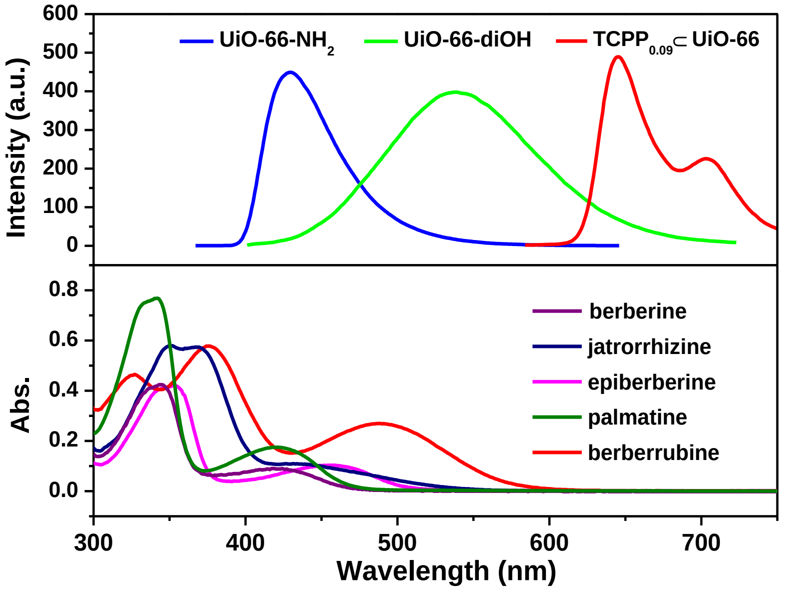

Fig. S10 Comparison of the emission spectra of luminescent ligands in MOF backbones with the absorption spectra of berberine homologues.

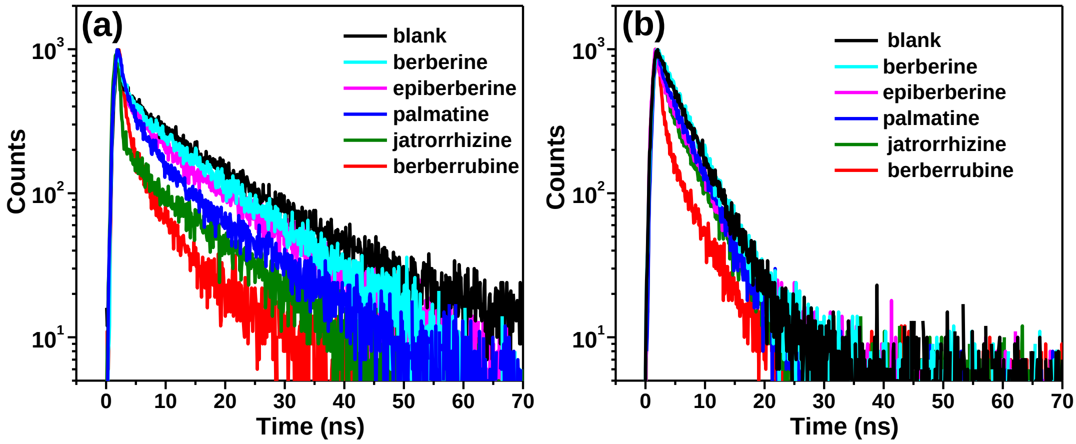

Fig. S11 Time-resolved decays of the emission bands at (a) 440 and (b) 536 nm upon the exposure of TCPP$_{0.09}$⊂UiO-66-(NH$_2$)$_{0.62}$(diOH)$_{0.38}$ to berberine homologues.

After the addition of berberine, epiberberine, palmatine, jatrorrhizine and berberrubine, the lifetime at 440 nm was shortened from the original value of 13.76 ns to 13.32, 12.66, 11.65, 10.10 and 7.28 ns, respectively. The lifetime of the emission band at 536 nm was nearly unchanged from the original value of 4.84 ns to 4.92, 4.72, 4.44, 4.26 and 3.58 ns, respectively.

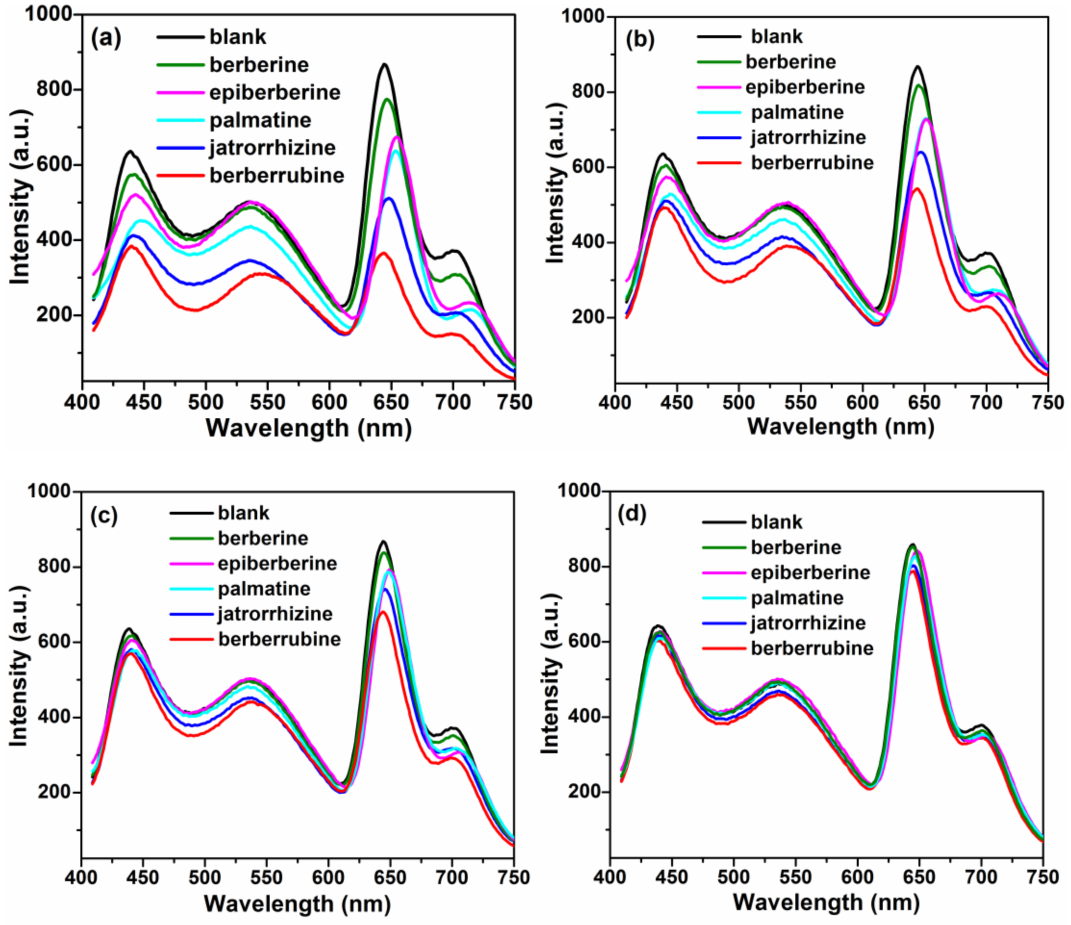

Fig. S12 Fluorescent spectra of TCPP$_{0.09}$⊂UiO-66-(NH$_2$)$_{0.62}$(diOH)$_{0.38}$ (50 mg L^{-1}) in the presence of berberine homologues with the concentrations of (a) 20, (b) 10, (c) 5 and (d) 2 μM.

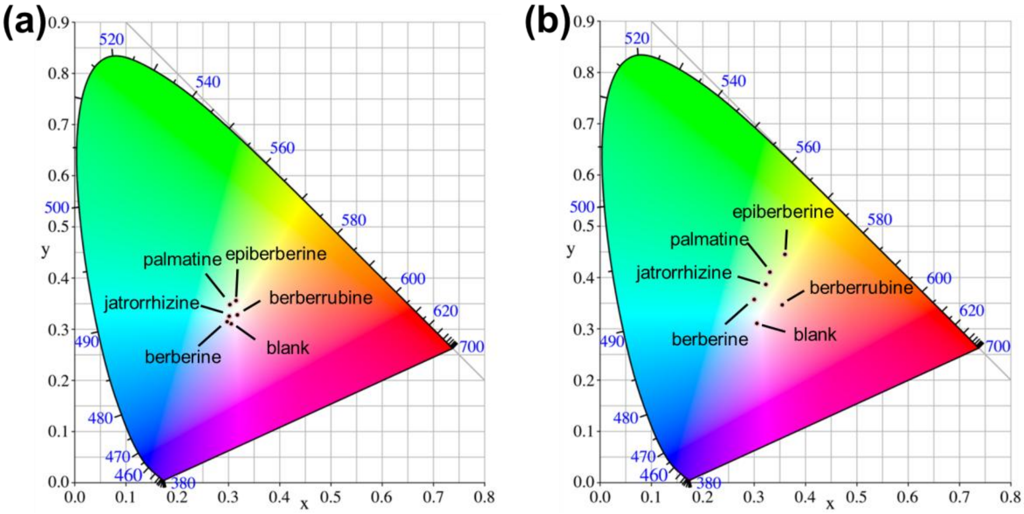

Fig. S13 CIE chromaticity diagrams of $TCPP_{0.09}\subset UiO\text{-}66\text{-}(NH_2)_{0.62}(diOH)_{0.38}$ in the presence of (a) 50 and (b) 200 μM berberine homologues.

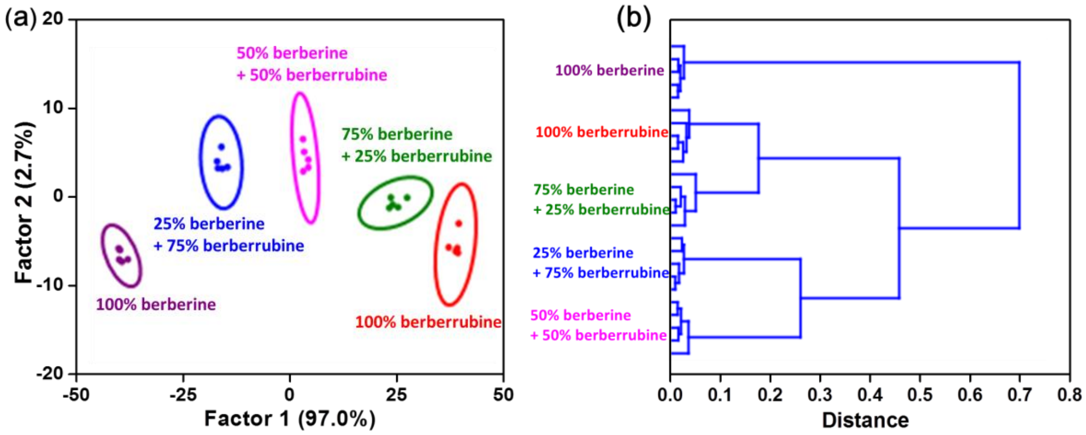

Fig. S14 (a) LDA and (b) HCA plots for $TCPP_{0.09}\subset UiO\text{-}66\text{-}(NH_2)_{0.62}(diOH)_{0.38}$ against the mixtures of berberine and berberrubine, $c_{\text{berberine}} + c_{\text{berberrubine}}$ = 50 μM.

Table S1 Compositions and CIE coordinates of synthesized MOF samples

Addition amount in synthesis (mmol)			Molar ratio of BDC-NH$_2$: BDC-diOH : TCPP in MOFs	CIE coordinates
H$_2$BDC-NH$_2$	H$_2$BDC-diOH	H$_4$TCPP		
0.150	0	0	1 : 0 : 0	(0.1540, 0.0564)
0.125	0.025	0	0.72 : 0.28 : 0	(0.1998, 0.1792)
0.120	0.030	0	0.69 : 0.31 : 0	(0.2187, 0.2211)
0.112	0.038	0	0.62 : 0.38 : 0	(0.2470, 0.2836)
0.100	0.050	0	0.52 : 0.48 : 0	(0.2850, 0.3662)
0.075	0.075	0	0.37 : 0.63 : 0	(0.3041, 0.4164)
0	0.150	0	0 : 1 : 0	(0.3492, 0.5197)
0.112	0.038	0.003	0.62 : 0.38 : 0.014	(0.2595, 0.2965)
0.112	0.038	0.006	0.64 : 0.36 : 0.036	(0.2686, 0.3019)
0.112	0.038	0.009	0.65 : 0.35 : 0.060	(0.2754, 0.3033)
0.112	0.038	0.012	0.63: 0.37 : 0.076	(0.2858, 0.3052)
0.112	0.038	0.015	0.65: 0.35 : 0.091	(0.3012, 0.3063)
0.112	0.038	0.018	0.65: 0.35 : 0.098	(0.3349, 0.3135)
0.112	0.038	0.021	0.65: 0.35 : 0.107	—

Table S2 Spectral overlap integrals of the emission of UiO-66-NH$_2$ with the absorptions of berberine homologues

	berberine	epiberberine	palmatine	jatrorrhizine	berberrubine
J^a	3.74×10^{13}	5.67×10^{13}	7.28×10^{13}	7.41×10^{13}	1.65×10^{14}

[a] The spectral overlap integral (J) is calculated with the equation of[1]

$$J = \int \overline{f_{\mathrm{D}}}(\lambda)\varepsilon_{\mathrm{A}}(\lambda)\lambda^4 \mathrm{d}\lambda$$

where $\overline{f}_{\mathrm{D}}$ is the donor (UiO-66-NH$_2$) emission spectrum normalized to an area of 1, and ε_{A} is the acceptor (berberine homologue) molar extinction coefficient obtained from the absorption spectrum.

Table S3 Training matrix of the fluorescent response (1 − I/I_0) patterns of $TCPP_{0.09}\subset UiO\text{-}66\text{-}(NH_2)_{0.62}(diOH)_{0.38}$ (50 mg L^{-1}) against alkaloids (50 µM)

Analyte	440 nm	536 nm	645 nm
berberine	0.173	0.052	0.202
	0.185	0.068	0.219
	0.175	0.013	0.212
	0.168	0.062	0.213
	0.165	0.053	0.219
jatrorrhizine	0.608	0.546	0.657
	0.611	0.540	0.661
	0.598	0.541	0.653
	0.619	0.549	0.669
	0.602	0.532	0.660
epiberberine	0.331	-0.015	0.502
	0.344	-0.010	0.527
	0.330	-0.007	0.514
	0.320	-0.009	0.524
	0.339	-0.013	0.526
palmatine	0.528	0.244	0.533
	0.513	0.243	0.525
	0.509	0.259	0.532
	0.520	0.256	0.550
	0.533	0.276	0.509
berberrubine	0.681	0.662	0.808
	0.660	0.673	0.815
	0.672	0.672	0.837
	0.694	0.661	0.798
	0.671	0.670	0.818
arecoline	0.019	0.017	0.019
	0.018	0.009	0.020
	0.028	0.018	0.016
	0.025	0.015	0.026
	0.020	0.011	0.019
theophyline	0.021	0.018	0.020
	0.022	0.015	0.028
	0.022	0.024	0.017
	0.026	0.014	0.018
	0.025	0.021	0.017
reserpine	0.009	0.014	0.012
	0.011	0.014	0.021
	0.010	0.017	0.015
	0.013	0.011	0.019
	0.008	0.011	0.010
quinine	0.035	0.031	0.041

	0.031	0.032	0.054
	0.035	0.028	0.039
	0.034	0.029	0.045
	0.032	0.034	0.048

Table S4 Jackknifed classification matrix of LDA in the differentiation of berberine homologues

Actual	Predicted					
	berberine	jatrorrhizine	epiberberine	palmatine	berberrubine	Total
berberine	5	0	0	0	0	5
jatrorrhizine	0	5	0	0	0	5
epiberberine	0	0	5	0	0	5
palmatine	0	0	0	5	0	5
berberrubine	0	0	0	0	5	5
Total	5	5	5	5	5	25

Table S5 Identification of 15 berberine homologue samples with unknown concentrations

Sample	Actual	Concentration (mM)		Fluorescent response ($1 - I/I_0$)			Predicted
		Added	Measured	440 nm	536 nm	645 nm	
1	berberine	0.80	0.73	0.165	0.052	0.184	berberine
2	jatrorrhizine	0.80	0.76	0.605	0.528	0.657	jatrorrhizine
3	epiberberine	0.80	0.72	0.301	-0.012	0.525	epiberberine
4	palmatine	0.80	0.84	0.491	0.232	0.557	palmatine
5	berberrubine	0.80	0.75	0.646	0.623	0.835	berberrubine
6	berberine	1.00	0.93	0.163	0.055	0.202	berberine
7	jatrorrhizine	1.00	0.98	0.646	0.512	0.695	jatrorrhizine
8	epiberberine	1.00	0.87	0.295	-0.013	0.498	epiberberine
9	palmatine	1.00	0.94	0.524	0.216	0.525	palmatine
10	berberrubine	1.00	1.06	0.683	0.649	0.854	berberrubine
11	berberine	1.20	1.10	0.152	0.059	0.214	berberine
12	jatrorrhizine	1.20	1.29	0.605	0.489	0.667	jatrorrhizine
13	epiberberine	1.20	1.08	0.293	-0.017	0.512	epiberberine
14	palmatine	1.20	1.32	0.564	0.287	0.608	palmatine
15	berberrubine	1.20	1.14	0.625	0.616	0.785	berberrubine

References

1. L. Yuan, W. Lin, K. Zheng and S. Zhu, *Acc. Chem. Res.*, 2013, **46**, 1462−1473.